



# A DISCUSSION ON THE APPLICATION OF BI-DIMENSIONAL SHAPE FACTORS OF PARTICLES CAUSING SEVERE WEAR OF METALS\*

*Giuseppe Pintaude<sup>1</sup>  
Mario Coseglio<sup>2</sup>*

## **Abstract**

The use of two-dimensional shape parameters to characterize abrasive particles is a possible approach to express their angularity. Nonetheless, in sliding abrasion, especially in pin abrasion testing, coated papers structure plays an important role and even its damage during the wear process should not be neglected. This manuscript discuss the limitations of two-dimensional shape descriptors in distinguishing wear caused by relatively hard particles, indicating that the wear data obtained in sliding abrasion tests are unable to distinguish different types of coated papers used when only the two-dimensional particle projection is considered for shape characterization.

**Keywords:** Wear; Particle shape; Sliding abrasion.

<sup>1</sup> *Dr. of Engineering, Professor, Programa de Pós-Graduação em Engenharia Mecânica e de Materiais, UTFPR, Curitiba, PR, Brazil.*

<sup>2</sup> *Master of Engineering, Lecturer, Programa de Pós-Graduação em Engenharia Mecânica e de Materiais, UTFPR, Curitiba, PR, Brazil.*

---

\* *Technical contribution to the 2<sup>nd</sup> International Brazilian Conference on Tribology – Tribology 2014, November 3<sup>rd</sup> to 5<sup>th</sup>, 2014, Foz do Iguaçu, PR, Brazil.*



## 1 INTRODUCTION

Wear caused by hard particles is strongly affected by the particle shape. This influence is considered in the model described by Rabinowicz *et al* [1]. This simple model was set up to explain the experimental results obtained and suggests that the wear rate per unit sliding,  $W$ , is directly proportional to the applied load  $F$  and vary inversely with surface hardness  $H$ , as indicated in Equation 1. The shape is included by representing the abrasive particle as idealized circular conical indenter with semi-apex angle  $\theta$ .

$$W = F(\overline{\cot\theta})/(\pi H) \quad (1)$$

Additional theoretical evidence of the importance of particle geometry representation by tridimensional objects is the definition of ploughing component of friction,  $\mu_p$ , proposed by Goddard and Wilman [2]. For idealized conical particles, for example, the ploughing component is defined in Equation 2), where  $p_m$  is the maximum flow pressure of the surface region of the abraded metal,  $p'_m$  is the dynamic pressure of the metal and  $\theta$  is the semi-apex angle of the conical idealized particle.

$$\mu_p = (2/\pi)(p'_m/p_m) \cot\theta \quad (2)$$

The measurement of attack angle, defined as the angle between the abrasive surface and the abraded surface, is a complex task in systems containing multiple particles. Hence, indirect ways to estimate it have been used, including surface roughness of worn surfaces [3] and two-dimensional shape parameters [4]. This work discuss the validity of two-dimensional shape parameters applicability in describing severe wear in pin abrasion tests, presenting which aspects of this type of tribosystem cannot be correlated with 2D descriptors.

## 2 USEFUL DEFINITIONS OF SHAPE PARAMETERS

Three definitions are presented here and used to characterize abrasive particles. A usual description of particle shape is based on how the particle projection differs from a circle. According to Wojnar [5], particle projections can be grouped in three families of shape according to their transition from a initial circle. The first case corresponds to ellipses with different elongations (Figure 1a) and the second represents the conditions where the shape remains rounded while the boundary irregularity increases (Figure 1b). The last case is a combination of the previous, i.e., the particle shape is far from a circle and has a complex boundary (Figure 1c). For each situation it is assumed that there is a most suitable descriptor to characterize the particle shape.

---

\* Technical contribution to the 2<sup>nd</sup> International Brazilian Conference on Tribology – TriboBR 2014, November 3<sup>rd</sup> to 5<sup>th</sup>, 2014, Foz do Iguaçu, PR, Brazil.

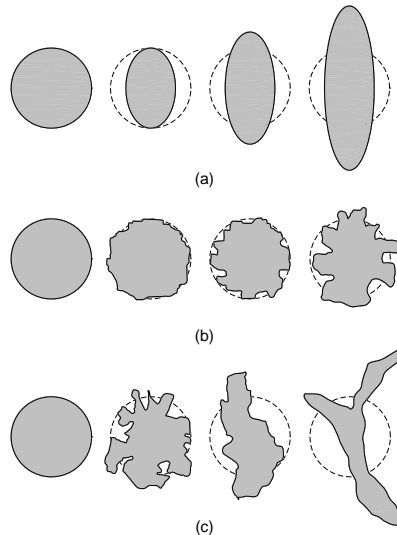


**Figure 1.** Particle shape comparison with a circle: (a) ellipses with different elongations; (b) increase in the border irregularity of rounded shapes; (c) combination of the previous cases. Adapted from Wojnar [5].

## 2.1 Aspect Ratio

The elongation presented in Figure 1a is very common in nodular particles plastically deformed due to the action of axial stresses, for example. An efficient manner to measure the elongation is the aspect ratio, usually defined as the ratio between the maximum length (e.g. maximum Feret diameter) and the corresponding width of the two-dimensional projection image of the particle (Equation 3).

$$A. R. = \frac{\max \text{Feret diameter}}{\text{width}} \quad (3)$$

The Heywood's elongation ratio is a similar shape descriptor which also correlates the particle length and width. In some terminologies, both parameters have no differentiation. The aspect ratio definition is illustrated in Figure 2.

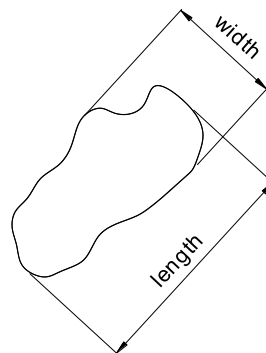


**Figure 2.** Aspect ratio definition.

## 2.2 Shape factor

Shape factor is one of the most used parameters to characterize the shape of abrasive particles. It is defined as the ratio between the particle projection area,  $A$ , and the area of the corresponding circle whose perimeter  $L$  equals the particle perimeter (Equation 4).

$$S. F. = (4\pi A)/(L^2) \quad (4)$$

\* Technical contribution to the 2<sup>nd</sup> International Brazilian Conference on Tribology – TriboBR 2014, November 3<sup>rd</sup> to 5<sup>th</sup>, 2014, Foz do Iguaçu, PR, Brazil.

This factor seems to be a good solution to define the case shown in Figure 1b. In these cases, when the particle is rounded, the factor is sensible to border irregularities. As the particle projection becomes circular the shape factor approaches 1 and as the border becomes irregular, its value decreases, as schematically illustrated in Figure 3.

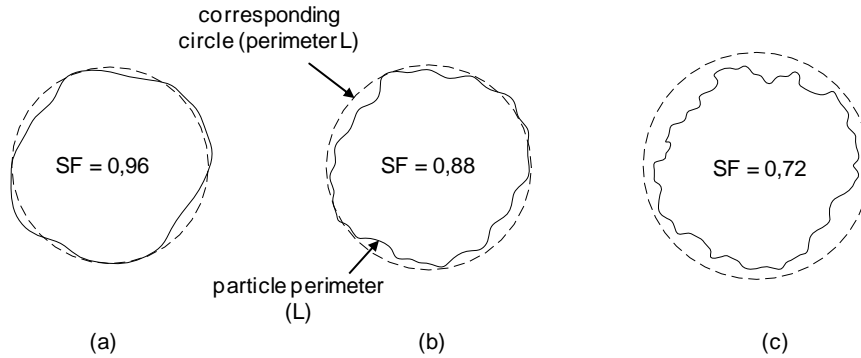


**Figure 3.** Particle irregularity detection by shape factor.

### 2.3 Spike Parameters

Two parameters were introduced by Hamblin and Stachowiak [6] to describe the particle angularity. The spike parameter (SP) is based on the projection particle boundary representation by a series of triangles at different scales. It is assumed that the smaller the apex angle and the higher the triangle size, the higher the particle abrasivity. In order to characterize both the angularity and the size, the spike value of each triangle ( $sv$ ) is defined according to Equation 4, where  $\phi$  is the apex angle and  $h$  is the triangle height (Figure 4).

$$sv = \cos(\phi/2)h \quad (4)$$

For each triangle found, the maximum spike value ( $sv_{max}$ ) is determined in terms of maximum triangle height ( $h_{max}$ ). The procedure is repeated for different step sizes along the perimeter and for all possible starting points at the border, resulting in an average spike value. The parameter is then determined by Equation 5, where  $m$  is the number of valid  $sv$  for a given step size and  $n$  is the number of different step sizes considered.

$$SP = (1/n) \sum [(1/m) \sum (sv_{max}/h_{max})] \quad (5)$$

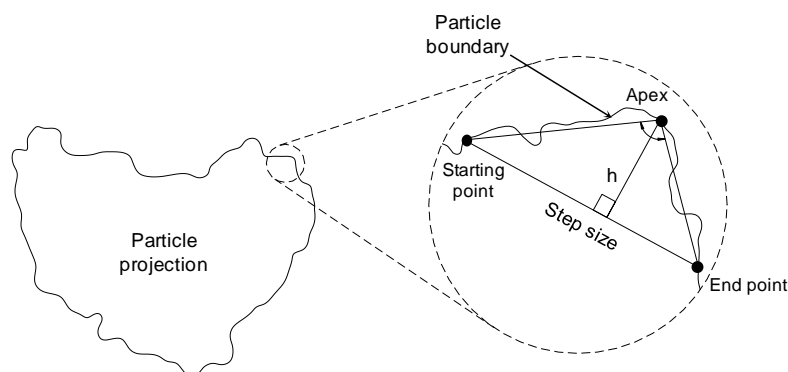


**Figure 4.** SP calculation procedure. Adapted from [6].

\* Technical contribution to the 2<sup>nd</sup> International Brazilian Conference on Tribology – TriboBR 2014, November 3<sup>rd</sup> to 5<sup>th</sup>, 2014, Foz do Iguaçu, PR, Brazil.

The second parameter proposed later by Hamblin and Stachowiak [7], named spike parameter – quadratic fit (SPQ), was developed to quantify particle angularity by detecting geometries potentially favorable for material removal process. The SPQ procedure is schematically represented in Figure 5.

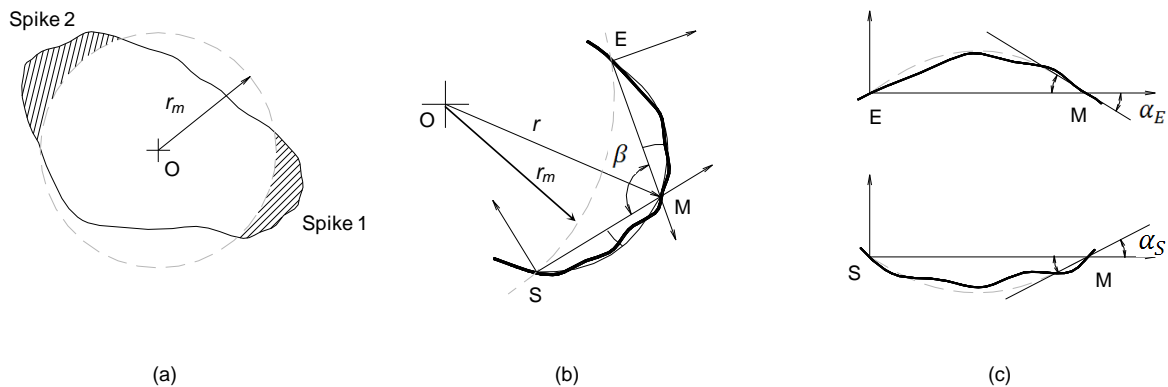


**Figure 5.** SPQ calculation procedure: (a) centroid location and  $r_m$  definition; (b) detail of spike 1; (c) side angles. Adapted from [8].

The first step consists in particle centroid localization (point  $O$ ). A circle with center at  $O$  and radius  $r_m$  is positioned, where the radius is determined by averaging all local radius ( $r$ ) along the particle boundary. Each region outside this circle or “spike” is characterized by the spike value ( $svq$ ) defined in Equation 6.

$$svq = \cos(\varphi/2) \quad (6)$$

The apex angle,  $\varphi$ , is composed of one central angle ( $\beta$ ) and two side angles ( $\alpha_S$  and  $\alpha_E$ ). The particle boundary portions between the segments SM and EM are approximated as polynomial functions and the side angles are then obtained by differentiating these functions at M. The SPQ is then obtained by the average value of all valid spike values found for the particle (Equation 7). The lower the apex angle the higher the spike value and, consequently, the higher the SPQ and the particle abrasivity.

$$SPQ = (1/n) \sum_{i=1}^n (svq_i) \quad (7)$$

### 3 EXPERIMENTAL

Two samples of alumina and glass particles were extracted from #80 mesh papers. Twenty particles whose average size are  $360 \pm 50 \mu\text{m}$  (alumina) and  $460 \pm 80 \mu\text{m}$  (glass) were randomly selected. Considering some previous results [8, 9], we can sustain that the particle size does not influence the two-dimensional analysis of shape description and then the size effect can be omitted due to its minor significance for the purpose of the present discussion. The images obtained from optical microscope were submitted to threshold process to convert the grayscale image to binary (Figure 6). The output binary images has values of 1 (white) for all pixels in the input image with luminance greater than defined level and 0 (black) for all other pixels. The transition level was based on the images histogram. Using the Image-Pro Plus software, the average values of shape factor and aspect ratio were determined for each group of particles. SPQ was determined using a set of functions in MATLAB’s image processing toolbox and algorithms developed following Equation 7.

\* Technical contribution to the 2<sup>nd</sup> International Brazilian Conference on Tribology – TriboBR 2014, November 3<sup>rd</sup> to 5<sup>th</sup>, 2014, Foz do Iguaçu, PR, Brazil.

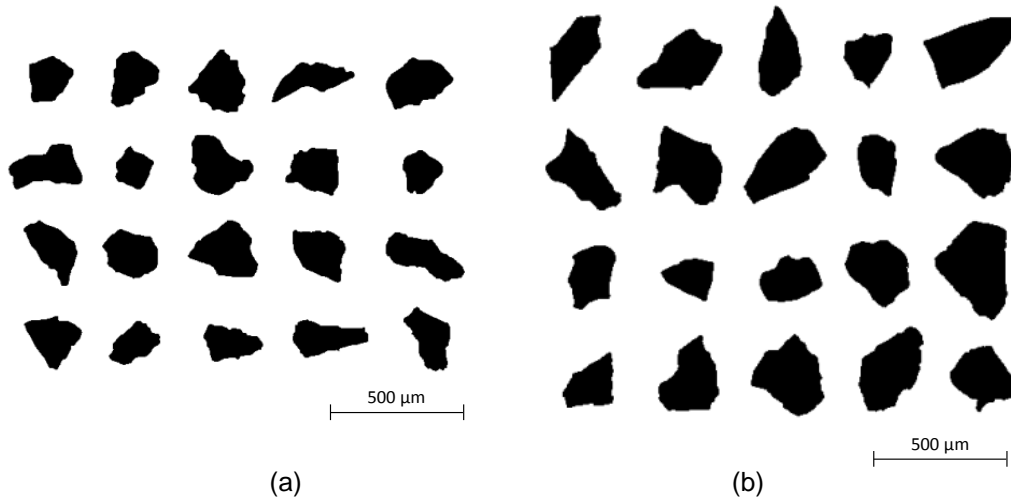


**Figure 6.** Binary images of abrasive particles for calculation procedure of shape factors: (a) alumina, (b) glass paper.

#### 4 RESULTS AND DISCUSSION

Table 1 shows the values of shape descriptors for glass and alumina particles removed from coated papers.

**Table 1.** Shape descriptors values for particles removed from coated papers.

Particle	SPQ	Shape Factor	Aspect Ratio
Glass	0.43±0.15	0.7±0.2	1.5±0.3
Alumina	0.37±0.15	0.7±0.1	1.6±0.5

None of shape descriptors were able to differentiate into glass or alumina particles, since all average values are significantly similar. These results open a possibility to affirm that their manufacturing processes were similar. Garboczi *et al.* [10], for example, did not find differences in shape of some rocks, which can indicate that blasting and crushing processes applied to produce them are based on the same breakage mechanism.

In terms of wear behavior, the results of Table 1 creates an expectation of similar wear rates when these particles abraded a same material keeping constant other system variables, following Equations 1 and 2. On the other hand, similar results of shape characterization may mean that two-dimensional approach does not work to explain wear results. These limitations were already discussed by Pintaude [9], who compared wear results produced by different abrasive sizes with similar shape parameters, which did not differentiate the wear rates. The limitation of two-dimensional characterization was also discussed here, based on results extracted from systems where the hardness of abrasive was much higher than worn material hardness.

We will discuss the application of two-dimensional shape parameters presented in Table 1 for pin abrasion testing using the results of wear and friction coefficients obtained by Pintaude *et al.* [11,12], presented in Table 2. As the particle geometry affects the cutting efficiency, besides the friction coefficient and the wear volume per sliding distance for each tribological system, the relation between the shape factor and the cutting efficiency should be discussed and it will be made using the abrasion factor. The definition of the abrasion factor,  $f_{ab}$ , is based on Figure 7.

\* Technical contribution to the 2<sup>nd</sup> International Brazilian Conference on Tribology – TriboBR 2014, November 3<sup>rd</sup> to 5<sup>th</sup>, 2014, Foz do Iguaçu, PR, Brazil.



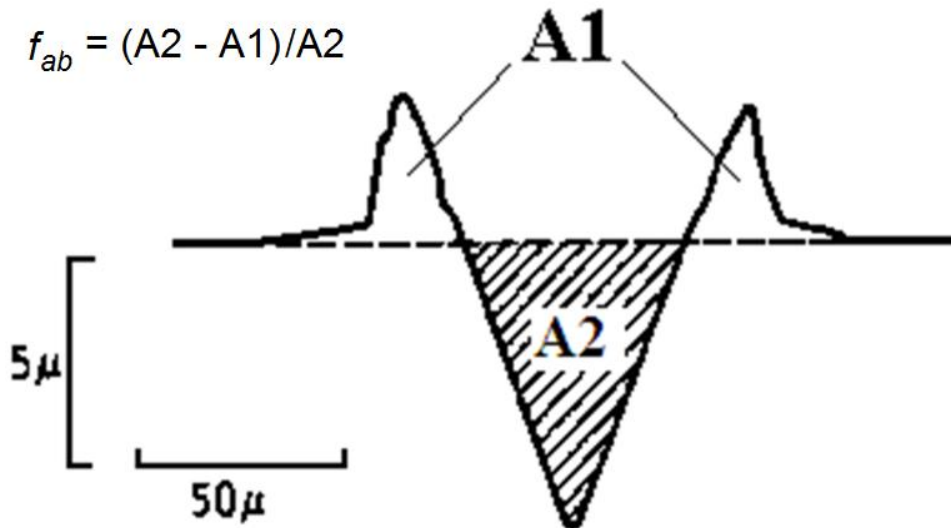


**Figure 7.** Definition of abrasion factor,  $f_{ab}$ . A1: the cross section area relative to pileup produced by a single scratch and; A2: the cross section area relative to the groove produced by a single scratch.

The abrasion factor defines the proportion of cutting micro-mechanism of abrasion. An alternative way to determine it is presented in [13], defined in (8):

$$f_{ab} = K/\mu_p \quad (8)$$

where  $K$  is the wear coefficient and  $\mu_p$  is the ploughing component of the friction coefficient. To determine  $\mu_p$ , the adhesive component of the friction coefficient is assumed as 0.2 [14], so that this value is reduced from the whole friction coefficient value. For both systems presented in Table 2 the constant value of  $\mu_p$  will be considered, once the formulation described in reference [14] did not consider the composition of tribological pairs.

**Table 2.** Severe wear indicators for different tribological pairs.

Tribological Pair*	Ha/H	Friction Coefficient	Wear volume per sliding distance ( $\text{m}^3/\text{m} \times 10^{-10}$ )	Abrasion factor, $f_{ab}$ (Eq.8)
Glass abraded 1006 steel [11]	5.7	0.53	2.80	0.04
Alumina abraded 1070 steel [12]	2.9	0.55	2.95	0.26

\*Both tests were performed using 20N. Ha: abrasive hardness, H: abraded metal hardness.

From Table 2, one can observe that both wear volume per sliding distance and friction coefficient can be considered similar, despite the variation of tribological pairs. Considering the Ha/H ratio as an indicative of wear severity, the values indicate an occurrence of severe wear mode, where microcutting is the main mechanism of material removal, described elsewhere in [11,12].

The similarity observed in tribological outputs for different systems was not enough to find very different values of abrasion factor. In part, it can be explained by the difference in worn material hardness, once the 1070 quenched and tempered steel is six times harder than 1006. It is well-known the effect of hardness of worn material on abrasion factor, when the wear is caused by relatively hard particles, i.e., the

\* Technical contribution to the 2<sup>nd</sup> International Brazilian Conference on Tribology – TriboBR 2014, November 3<sup>rd</sup> to 5<sup>th</sup>, 2014, Foz do Iguaçu, PR, Brazil.



harder the particle material, the higher the abrasion factor. In addition, the abrasion factor is influenced by particle geometry, such that sharp contacts lead to high values of  $f_{ab}$ .

An important observation can be made based on surface images of abrasive papers providing by Coronado *et al.* [15]. They performed wear tests using SiC, alumina, garnet and glass papers with average size between 60 and 66  $\mu\text{m}$ . When one observes the surfaces of the coated papers supplied by these researchers, it is worthwhile the big difference in the particle morphology found in glass paper. In this case, the two-dimensional approach to characterize the geometry of abrasive particles does not capture the coated structure of papers, which in fact perform the effective contact with the tested surface.

The average values of shape parameters of twenty particles of glass and alumina particles provided by Coronado *et al.* [15] were calculated and they are presented in Table 3.

**Table 3.** Shape descriptors values for coated papers revealed by [15].

Particle	SPQ	Shape factor	Aspect Ratio
Glass	0.5±0.1	0.7±0.1	1.7±0.5
Alumina	0.5±0.2	0.7±0.1	1.9±0.6

As already observed in Table 1, again none of shape descriptors were able to distinguish between glass and alumina particles in terms of angularity, even considering that their surface images are quite different. A significant aspect observed under glass coated paper is the presence of relatively free particles. These particles can become into three body agents during the wear process, a phenomena already described in [11]. This occurrence increases the abrasive-abrasive contacts, changing the values of friction components, and consequently, the value of abrasion factor calculated by Equation 8.

Besides the discussion on structure of coated papers, another relevant effect is usually reported in pin abrasion testing: the loading of the abrasive papers, where debris are entrapped into space among abrasive grains. This effect is more pronounced for soft metals and it was reported in the case of 1006 steel [11]. A consequence is the increase in metal-metal contacts, leading to changes on the adhesive component of friction. In addition, and probably more important for this discussion, the effective geometry of abrasive in contact with the worn surface is very different of the free and removed grain of coated paper. When this effect is observed, the use of a constant value for adhesive component of friction to calculate the abrasion factor is not more possible. As a consequence, the value of the abrasion factor following Equation 8 is also altered.

## 4 CONCLUSIONS

From the above discussed results, the following conclusions can be presented:

- Two-dimensional approach to characterize particle geometry does not capture three body abrasion effects neither tribolayer formation during wear process. In this way, its application is not recommended for sliding abrasion systems, in particular those made use of pin abrasion testing with coated papers.
- The use of adhesion component of friction as a constant to determine abrasion factor only can be applied in cases with no particle degradation, such as in system employing loading paper.

\* Technical contribution to the 2<sup>nd</sup> International Brazilian Conference on Tribology – TriboBR 2014, November 3<sup>rd</sup> to 5<sup>th</sup>, 2014, Foz do Iguaçu, PR, Brazil.





## Acknowledgments

G. Pintaude acknowledges CNPq by granting from Project 306727/2011-0.

## REFERENCES

- 1 Rabinowicz E, Dunn L A; Russell PG. A study of abrasive wear under three-body conditions. *Wear*. 1961;4(5):345-355.
- 2 Goddard, J.; Wilman, H. A theory of friction and wear during the abrasion of metals. *Wear*. 1962; 5(2):114-135.
- 3 Spurr, R. T. The nature of contact during abrasion. *Wear*. 1981; 67(3):375-379.
- 4 Stachowiak, G. W. Particle angularity and its relationship to abrasive and erosive wear. *Wear*. 2000; 241(2):214-219.
- 5 Wojnar L. *Image Analysis: Applications in Materials Engineering*. Boca Raton: CRC Press; 1999.
- 6 Hamblin MG, Stachowiak GW. A multi scale of particle abrasivity. *Wear*. 1995; 183:225-233.
- 7 Hamblin MG, Stachowiak GW. Description of abrasive particle shape and its relation to two-body abrasive wear. *Tribology Transactions*. 1996; 39: 803-810.
- 8 Coseglio M, Pintaude G. Abrasive Particle Characterization Following Different Measurements of Shape Factor. In: 20th International Congress of Mechanical Engineering, 2009, Gramado. *Proceedings of COBEM 2009*. Rio de Janeiro: ABCM, 2009.
- 9 Pintaude G. Characteristics of Abrasive Particles and Their Implications on Wear. In: Taher Ghrib (Ed.). (Org.). *New Tribological Ways*. 1ed.: Intech, 2011, p. 117-130.
- 10 Garboczi EJ, Liu X, Taylor MA. The 3-D shape of blasted and crushed rocks: From 20 $\mu$ m to 38mm. *Powder Technol*. 2012;229:84-89.
- 11 Pintaude G, Tanaka DK, Sinatora, A. The effects of abrasive particle size on the sliding friction coefficient of steel using a spiral pin-on-disk apparatus. *Wear*. 2003;255: 55-59.
- 12 Pintaude G, Bernardes FG, Santos MM, Sinatora A, Albertin E. Mild and severe wear of steels and cast irons in sliding abrasion, *Wear*. 2009;267: 19-25.
- 13 Jacobson S, Wallén P, Hogmark S. Fundamental aspects of abrasive wear studied by a new numerical simulation model. *Wear*. 1988;123: 207-223.
- 14 Sin H, Saka N, Suh N P. Abrasive wear mechanisms and the grit size effect. *Wear*. 1979;55; 163-190.
- 15 Coronado JJ, Rodríguez SA, Sinatora A. Effect of particle hardness on mild-severe wear transition of hard second phase materials. *Wear*. 2013;301:82-88.

---

\* *Technical contribution to the 2<sup>nd</sup> International Brazilian Conference on Tribology – TriboBR 2014, November 3<sup>rd</sup> to 5<sup>th</sup>, 2014, Foz do Iguaçu, PR, Brazil.*